

MirrorVerse: Pushing Diffusion Models to Realistically Reflect the World

Ankit Dhiman^{1,2*} Manan Shah^{1*} R Venkatesh Babu¹

¹Vision and AI Lab, IISc Bangalore ²Samsung R & D Institute India - Bangalore

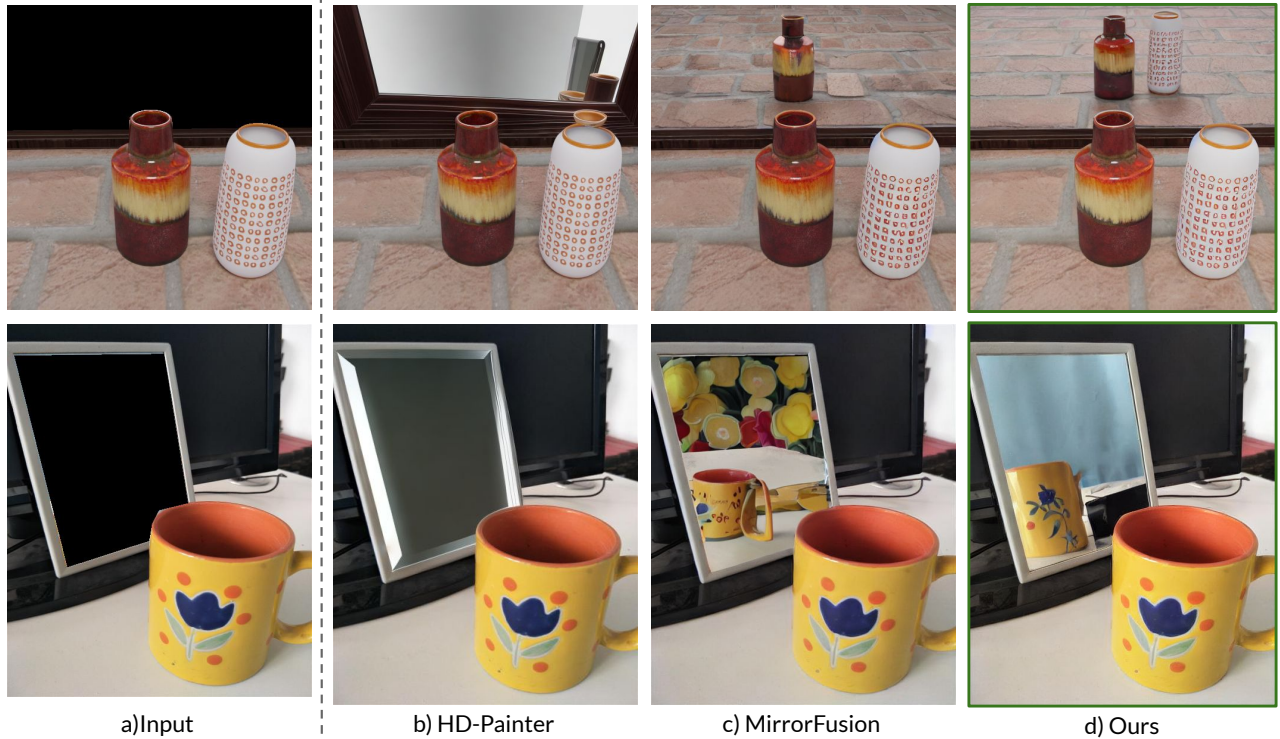


Figure 1. Our model MirrorFusion 2.0, trained on our enhanced dataset SynMirrorV2 surpasses previous state-of-the-art diffusion-based inpainting models at the task of generating mirror reflections. All images were created by appending the prompt: “A perfect plane mirror reflection of ” to the object description. All text prompts can be found in the supplementary.

Abstract

Diffusion models have become central to various image editing tasks, yet they often fail to fully adhere to physical laws, particularly with effects like shadows, reflections, and occlusions. In this work, we address the challenge of generating photorealistic mirror reflections using diffusion-based generative models. Despite extensive training data, existing diffusion models frequently overlook the nuanced details crucial to authentic mirror reflections. Recent approaches have attempted to resolve this by creating synthetic datasets and framing reflection generation as an inpainting task; however, they struggle to generalize across different object orientations and positions relative to the

mirror. Our method overcomes these limitations by introducing key augmentations into the synthetic data pipeline: (1) random object positioning, (2) randomized rotations, and (3) grounding of objects, significantly enhancing generalization across poses and placements. To further address spatial relationships and occlusions in scenes with multiple objects, we implement a strategy to pair objects during dataset generation, resulting in a dataset robust enough to handle these complex scenarios. Achieving generalization to real-world scenes remains a challenge, so we introduce a three-stage training curriculum to develop the MirrorFusion 2.0 model to improve real-world performance. We provide extensive qualitative and quantitative evaluations to support our approach. The project page is available at: <https://mirror-verse.github.io/>.

*Equal Contribution.



Figure 2. We observe that current state-of-the-art T2I models, SD3.5 [2] (top row) and Flux [22] (bottom row), face significant challenges in producing consistent and geometrically accurate reflections when prompted to generate reflections in the scene.

1. Introduction

In recent years, diffusion-based generative models have re-defined what is possible in fields spanning from image generation to video synthesis, producing impressive results across various applications [14, 17, 18, 22, 35, 38]. The evolution of these models has been accompanied by a range of methods designed to fine-tune the generation process through conditional inputs, such as edge maps, sketches, depth maps, and segmentation maps [30, 54, 56, 58]. However, there remains a significant gap in their capacity to replicate intricate physical effects—particularly those rooted in the subtlety of real-world physics, including shadows [41], specular reflections [49], and perspective cues [46]. More challenging still, these techniques struggle to authentically generate mirror reflections, a task requiring a nuanced understanding of light, geometry, and realism that current methods do not adequately address. In this work, we address the question: “*Can current methods be fine-tuned to generate plausible mirror reflections?*”

We motivate the problem further by providing generations from current text-to-image (T2I) generation models. We prompt Stable Diffusion 3.5 [2] and FLUX [22] with prompts to generate a scene with a mirror reflection. Fig. 2 shows that these methods fail to generate plausible mirror reflections. Specifically, check the reflection of “teddy-bear” in the generated outputs from both the methods. Further, inpainting methods like HD-Painter [27] also fail for this task, as shown in Fig. 1. A contemporary method called MirrorFusion [12], claiming to generate mirror reflections, falls short on real-world and challenging scenes as apparent in Fig. 1.

Despite their impressive capabilities, powerful diffusion models struggle to generate mirror reflections accurately.

Table 1. Our proposed dataset, **SynMirrorV2**, surpasses existing mirror datasets in terms of attribute diversity and variability. While recent work [12] introduced the synthetic SynMirror dataset, it lacks key augmentations and scenario, limiting its performance in complex and real-world settings (See Fig. 1).

| Dataset | Type | Size (#Images) | Attributes |
|---------------------------|--|----------------|---|
| MSD [52] | Real | 4,018 | RGB, Masks |
| Mirror-NeRF [55] | Real & Synthetic | 9 scenes | RGB, Masks, Multi-View |
| DLSU-OMRS [15] | Real | 454 | RGB, Mask |
| TROSD [44] | Real | 11,060 | RGB, Mask |
| PMD [24] | Real | 6,461 | RGB, Masks |
| RGBD-Mirror [28] | Real | 3,049 | RGB, Depth |
| Mirror3D [45] | Real | 7,011 | RGB, Masks, Depth |
| SynMirror [12] | Synthetic | 198,204 | Single Fixed Objects: RGB, Depth, Masks, Normals, Multi-View |
| SynMirrorV2 (Ours) | Synthetic with Single & Multiple Objects | 207,610 | Single + Multiple Objects : RGB, Depth, Masks, Normals, Multi-View, Augmentations |

This limitation stems from the models’ reliance on poorly learned priors, a consequence of the quality and quantity of their training data. The scarcity of high-quality, real-world images featuring mirrors and their reflections, as evidenced in Tab. 1, poses a significant challenge. While recent work [12] has attempted to address this issue by training on a synthetic dataset, the results, as illustrated in Fig. 1, suggest that the method’s performance suffers in complex scenes and real-world settings. We hypothesize that this is due to inherent limitations in the synthetic data generation process and the training dynamics of the model.

To address the shortcomings in the synthetic data generation pipeline, we create an enhanced pipeline incorporating useful augmentations such as randomizing object position and rotation. We also ensure that the objects are anchored to the ground level in the 3D world. We observe that this diverse data improves the generalization of a trained model across the pose and position of objects in the scene. However, it does not generalize to more complex scenes with multiple objects. To address this, we propose a novel pipeline that places multiple objects in the scene based on their semantic categories, further enhancing the quality and utility of the proposed synthetic dataset. Drawing inspiration from previous works, such as those that have improved the generation quality on various tasks, notably image-editing [29], multilingual T2I generation [23, 50, 53] and several others, we aim to leverage the stage-wise training approach that enhanced the results in these methods.

We briefly sum up our contributions as follows:

- We propose SynMirrorV2, a large-scale synthetic dataset with diversity in objects and their relative position and orientation in the scene.
- Further, we create a pipeline to add multiple objects to a scene in SynMirrorV2.
- We show that with a curriculum strategy of training on SynMirrorV2, a generative method can also generalize to real-world scenes. We show this generalization capability on the challenging real-world MSD [52] dataset.

2. Related Work

Image Generative models. Diffusion models [43] have become quite popular for image generation tasks. Diffusion models work by gradually adding noise to data and then learning to reverse this process to generate data from a variety of distributions [8, 11, 17]. Subsequent works have expanded the scope of image generation by incorporating text guidance [37, 40] into the diffusion process, simplifying the reverse process [48], and reformulating diffusion to occur in a latent space [38] for improved speed. [31] explore advancements in diffusion models by addressing bias through distribution-guided debiasing techniques. Further, methods [32, 33] are developed to provide more fine-grained generation control to these models. Building on the success of vision transformers [47], recent approaches [7, 34, 60] have replaced the U-Net architecture in diffusion models with transformer-based designs, leading to high-quality image generation results. Further, there are popular methods [2, 22] for high-quality image generation. However, these methods also fail for the task of generating reflections on the mirror as shown in Fig. 2

Image Inpainting. Building on the advancements in image diffusion models, methods like Palette [39] and Re-paint [26] leverage known regions through the denoising process to reconstruct missing parts. Blended Diffusion [3, 4] refines this approach by replacing noise in unmasked areas with known content but struggles with complex scenes and shapes. Stable-Diffusion Inpainting [38] (SDI) enhances results by fine-tuning the denoiser with noisy latents, masks, and masked images. Recent methods, such as HD-Painter [27], PowerPoint [61], SmartBrush [51] build on SDI with additional training. Recently, BrushNet [20] introduces a plug-and-play architecture that preserves unmasked content while improving coherence with textual prompts. However, Fig. 1 highlights the limitations of these methods in generating reflections on the mirror.

Diffusion Models and 3D concepts. Recently, LRM [19] based methods predict 3D model from a single image. Some methods [21] utilize diffusion-based methods to enable editing of these 3D presentations. Other diffusion-based methods [29] use synthetic image pairs for 3D-aware image editing. However, the synthetic-to-real domain gap can limit their applicability. Further, ObjectDrop [49] trains a diffusion model for object insertion/removal using a counterfactual dataset that can handle shadows and specular reflections. Sarkar et al. [41] shows that generated images have different geometric features such as shadows and reflections from the real images. Upadhyay et al. [46] proposed a geometric constraint in the training process to improve the perspective cues in the generated images. Alchemist [42] provides control over the material properties of an object by proposing an object-centric synthetic dataset with physically-based materials.

3. Dataset

3.1. Data Generation Pipeline

Fig. 2 highlights the failure of state-of-the-art models in handling the reflection generation task. MirrorFusion [12] addresses this challenge by proposing a synthetic dataset but struggles in complex scenarios involving multiple objects and real-world scenes (Fig. 1). We attribute this limitation to the lack of diversity in their dataset. To mitigate these shortcomings, we introduce SynMirrorV2, a large-scale dataset which significantly expands diversity with varied backgrounds, floor textures, objects, camera poses, mirror orientation, object positions, and rotations. Tab. 1 compares existing mirror datasets, while Fig. 3 showcases samples from SynMirrorV2.

Object Sources. We source objects from Objaverse [9] and Amazon Berkeley Objects (ABO) [6] datasets. Objaverse, a large-scale dataset, contains 800K diverse 3D assets, while ABO contributes 7,953 common household objects. To ensure quality, we refine our selection using a curated list of 64K objects from OBJECT 3DIT [29] and the filtering procedure discussed in [12], eliminating low-quality textures and sub-par renderings. After filtering, we get 58,109 objects from Objaverse. In total, we utilize 66,062 objects.

Scene Resources. To create a realistic scene, we require assets such as a mirror, floor and background. We create a plane for the floor and apply diverse textures sourced from CC-textures [10]. We use HDRI samples provided by PolyHaven [16] to represent the background. In our experiments, we use different kinds of mirrors: full-wall mirrors and tall rectangular mirrors. For lighting, we position an area-light slightly above and behind the object at a 45° angle, directing it towards both the object and the mirror.

Object Placement in the scene. To begin, we fix the mirror’s position within the scene as a fixed reference point. The sampled object is then scaled to fit within a unit cube, ensuring uniformity in size across all objects. We proceed by sampling the object’s x-y position from a pre-computed region that guarantees both visibility of the object in the mirror and camera. This pre-computed region is determined by identifying the intersection between the mirror’s viewing frustum and the camera’s viewing frustum. Once the position is set, we randomly sample an angle for the object’s rotation around the y-axis to introduce variability. However, even with these steps, there may be instances where the object appears to float in the air, which can undermine the dataset’s utility. To address this, we apply a straightforward grounding technique, detailed in the supplementary material. Together, these strategies contribute to the diversity and overall quality of the proposed dataset.

Multiple Objects. A typical scene includes multiple objects arranged in varied layouts, producing a range of depth and occlusion scenarios that enhance scene realism. To

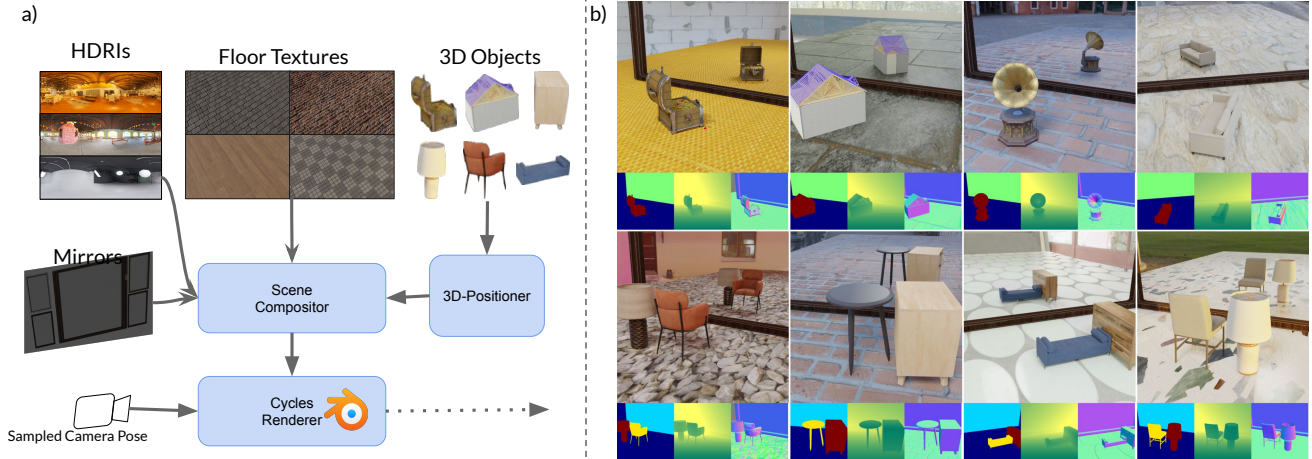


Figure 3. **Dataset Generation Pipeline.** Our dataset generation pipeline introduces key augmentations such as **random positioning, rotation, and grounding** of objects within the scene using the 3D-Positioner. Additionally, we pair objects in semantically consistent combinations to simulate complex spatial relationships and occlusions, capturing realistic interactions for **multi-object** scenes.

Algorithm 1 Procedure to Render Multiple Objects

Require: Input 3D model \mathcal{M}_1

- 1: **Function** GETPAIREDOBJECTCATEGORY(M)
- 2: $c \leftarrow$ GetSemanticCategory(M)
- 3: $L \leftarrow$ GetPairedCategoriesList(c)
- 4: $c_{paired} \leftarrow$ SampleCategory(L)
- 5: **return** c_{paired}
- 6: **Function** SAMPLEOBJECT(c)
- 7: $L_{obj} \leftarrow$ GetListObjects(c)
- 8: $\mathcal{M} \leftarrow$ Sample3DObject(L_{obj})
- 9: **return** \mathcal{M}

10: Main Algorithm

- 11: $c_{paired} \leftarrow$ GETPAIREDOBJECTCATEGORY(\mathcal{M}_1)
- 12: $\mathcal{M}_2 \leftarrow$ SAMPLEOBJECT(c_{paired})
- 13: Initialize position of \mathcal{M}_2 at X
- 14: **while** \mathcal{M}_2 collides with \mathcal{M}_1 **do**
- 15: $T_r \leftarrow$ SampleRandomPosition()
- 16: $X \leftarrow T_r$
- 17: **end while**

capture this complexity, our dataset incorporates scenes with multiple objects, as described in Algorithm 1. We start by sampling K objects from the original ABO dataset and identifying each object’s class from [6]. Categories are manually paired to ensure semantic coherence—for instance, pairing a chair with a table. During rendering, after positioning and rotating the primary object K_1 , an additional object K_2 from the paired category is sampled and arranged to prevent overlap, ensuring distinct spatial regions within the scene. This process yields 3,140 scenes featuring diverse object configurations and spatial relationships, providing a robust foundation for realistic scene representation.

Rendering. Following scene composition, we randomly sample three camera poses from a predefined list of 19 camera positions and render each scene using BlenderProc [10] to obtain RGB, depth, normal, and semantic label outputs. All renderings are produced at a resolution of 512×512 pixels. We set the “cycles rendering” parameter to 1024, which is necessary for accurately capturing reflections. Representative samples are provided in Fig. 3 and additional examples are available in the supplementary material.

4. Method

Preliminaries Diffusion models are generative models that can construct data samples by progressively removing noise. In the forward diffusion process, Gaussian noise $\epsilon \sim \mathcal{N}(0, 1)$ is incrementally added to an initial clean sample x_0 over T timesteps to create a noisy sample x_T . In the reverse process, a clean image x_0 is reconstructed by iteratively denoising x_T . This denoising process is carried out by a denoising network ϵ_θ which is conditioned on the timestep $t \in \{1, T\}$ and optional additional conditioning c (e.g. text prompts, inpainting masks). Training loss of the denoiser is as follows:

$$L_{DM} = E_{x_0, \epsilon \sim \mathcal{N}(0, I), t} \|\epsilon - \epsilon_\theta(z_t, t, c)\|^2 \quad (1)$$

Model Architecture. Building upon MirrorFusion [12], we also formulate this task as an inpainting task. Our model employs a base dual branch network similar to BrushNet [20] and additionally uses depth map conditioning for the condition branch of BrushNet. In particular, we concatenate the noisy latent z_t , masked image z_m , inpainting mask x_m and depth map x_d , and provide this as an input to

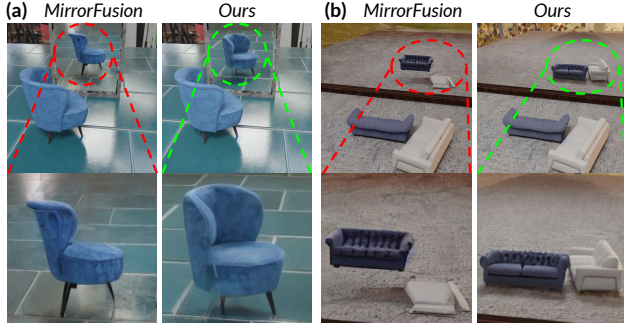


Figure 4. **Comparison on MirrorBenchV2.** The baseline fails to maintain accurate reflections and spatial consistency, showing (a) incorrect chair orientation and (b) distorted reflections of multiple objects. In contrast, our method correctly renders (a) the chair and (b) the sofas with accurate position, orientation, and structure, demonstrating superior performance.

the conditioning U-Net branch. Each layer of the generation U-Net ϵ_i is conditioned with the corresponding layer of the conditioning U-Net ϵ' with the help of zero-convolutions (\mathcal{Z}) as follows:

$$\epsilon_{\theta}(z_t, t, c)_i = \epsilon_{\theta}(z_t, t, c)_i + w \cdot \mathcal{Z} \left(\epsilon'_{\theta}([z_t, z_m, x_m, x_d], t)_i \right) \quad (2)$$

w is the preservation scale to adjust the influence of conditioning. We set w to be 1.0 for all our experiments. We, train the model with the loss in Eq. (1).

Training details. We follow a 3 stage training curriculum to improve the generalization of the model on real-world scenes. We utilize the AdamW [25] optimizer with a learning rate of $1e^{-5}$ and a batch size of 4 per GPU. We train on 4 NVIDIA A100 GPUs in all stages.

- **Stage 1.** In the first stage, we initialize the weights of both the conditioning and generation branch with the Stable Diffusion v1.5 checkpoint and finetune the model on the single object train split of our proposed SynMirrorV2. In contrast to [12], we do not keep the generation branch frozen and train the model till 40,000 iterations. The variation in the position and rotation in the SynMirrorV2 compared to SynMirror allows us to train the model for longer iterations without any degradation in the generation quality compared to [12].
- **Stage 2.** In the second stage, we finetune the model for 10,000 iterations on the multiple objects train split of SynMirrorV2 to incorporate the concepts of occlusions as present in realistic scenes.
- **Stage 3.** We propose a third stage training on real-world data from the MSD [52] dataset for another 10,000 iterations to bridge the domain gap between synthetic and real-world image inpainting.

In the first two stages, we use ground truth depth maps and for the third stage, we generate depth maps using a

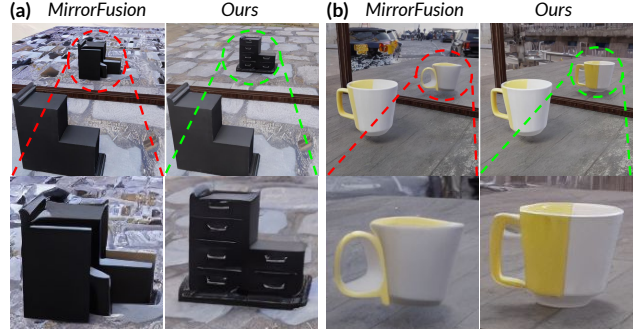


Figure 5. **Comparison on GSO [13] dataset.** In (a), the baseline method misrepresents object structure, while our method preserves spatial integrity and produces realistic reflections. In (b), the baseline yields incomplete and distorted reflections of the mug, whereas our approach generates accurate geometry, color, and detail, showing superior performance on out-of-distribution objects.

monocular depth estimator [5]. To enhance learning and reduce reliance on text prompts, we randomly drop them 20% of the time during training, enabling the model to utilize depth information better.

Inference. During inference, we use a CFG value of 7.5 and utilize the UniPC scheduler [59] for 50 time steps. During inference, we allow the user to provide the mask depicting the mirror and estimate the input depth map using Depth-Pro [5] by passing the masked image as input.

5. Experiments & Results

We discuss the evaluation strategy and compare our current method with the previous state-of-the-art method, MirrorFusion [12], referring to this as the baseline. Additionally, we also provide ablation studies on different design choices in Sec. 5.1.

Dataset. Compared to MirrorBench, MirrorBenchV2 consists of renderings of single and multiple objects in a scene. Additionally, we qualitatively test our method on several images from the MSD dataset and renderings from the Google Scanned Objects(GSO) [13] dataset. For single object renderings, we have a total of 2,991 images, which come from categories that are both seen and unseen during training. We create 300 images that contain two objects from the ABO dataset in the same scene to test the model on generating reflections for multiple objects.

Metrics. We benchmark various methods on the quality of the generated reflection and textual alignment of the generated image with the input prompt.

- **Reflection Generation Quality.** We evaluate reflection quality using Peak-Signal-to-Noise ratio (PSNR), Structural Similarity (SSIM) and Learned Perceptual Image Patch Similarity (LPIPS) [57] on the masked mirror region.

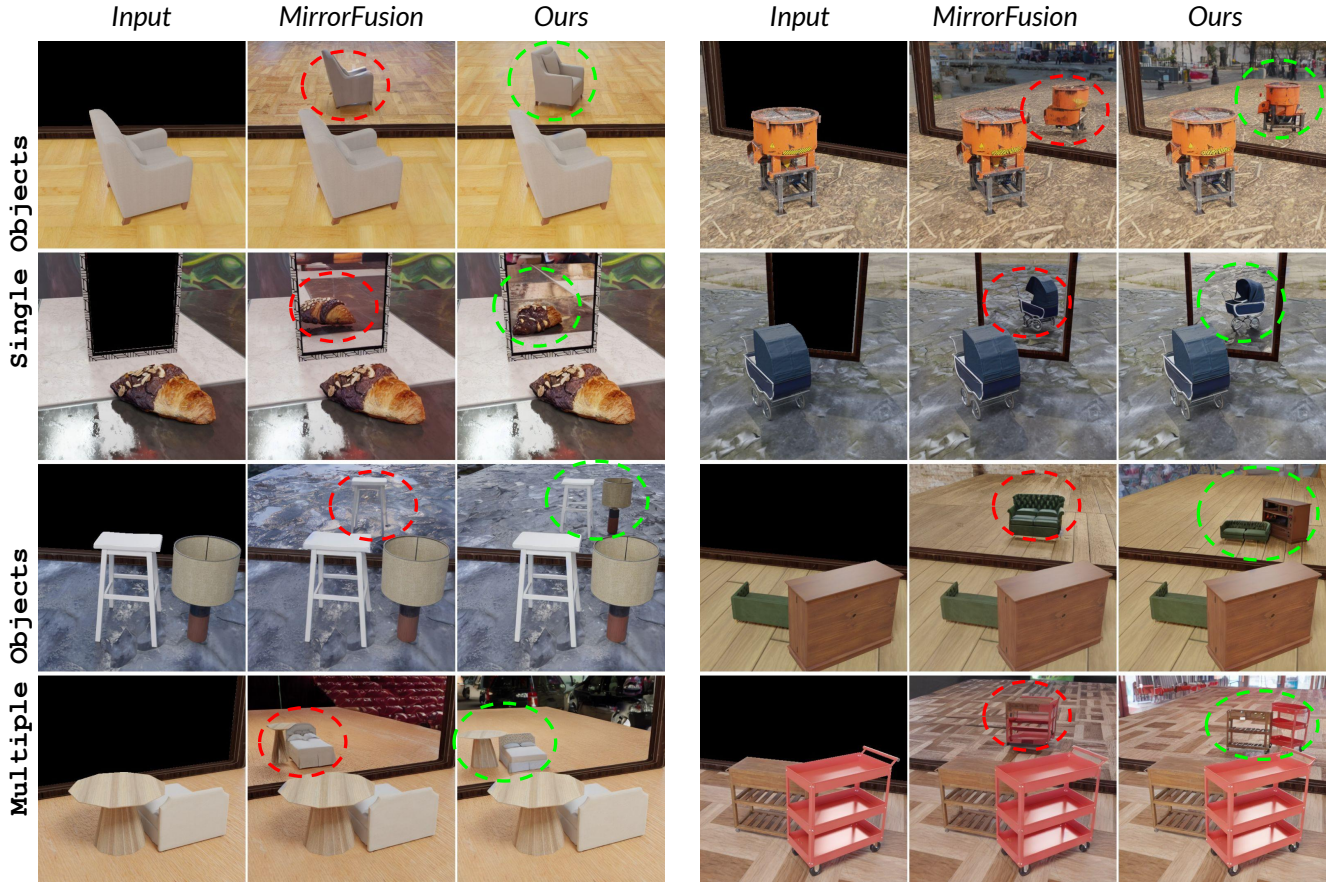


Figure 6. **Results on MirrorBenchV2.** We compare our method with the baseline MirrorFusion [12] on MirrorBenchV2. The baseline method shown struggles with pose variations, even in single-object scenes, and fails to produce accurate reflections for multiple objects. In contrast, our method handles variations in the object orientation effectively and generates geometrically accurate reflections, even in complex, multi-object scenarios.

- **Text Alignment.** We use CLIP [36] Similarity for assessing textual alignment.

Qualitative results on MirrorBenchV2. In Fig. 4 (a), a single chair that is slightly rotated is placed in front of a mirror. We observe that the baseline method completely misrepresents the chair’s orientation in the generated reflection as seen in the mirror. Notice the zoomed-in region where the reflection appears as if the object was cut and pasted onto the mirror. In contrast, MirrorFusion 2.0 trained on SynMirrorV2 accurately captures the chair’s orientation in the reflection, as shown in the zoomed-in region highlighted by the green circle.

Fig. 4 (b), shows a scene with a white sofa rotated and placed to the right of a gray sofa. The baseline method produces two artifacts in the reflection: 1) the gray sofa appears to be floating in the air, and 2) the generated reflection of the white sofa is completely incorrect. In contrast, our method accurately generates the scene in the reflection. These results demonstrate the effectiveness of our augmen-

tation strategies, as described in Sec. 3. We show more examples with both single and multiple objects in Fig. 6.

Qualitative results on GSO [13]. We further evaluate the generalization ability of MirrorFusion 2.0 on real-world scanned objects from GSO, shown in Fig. 5. MirrorFusion 2.0 generates significantly more accurate and realistic reflections. For instance, in Fig. 5 (a), MirrorFusion 2.0 correctly reflects the drawer handles (highlighted in green), while the baseline model produces an implausible reflection (highlighted in red). Likewise, for the “White-Yellow mug” in Fig. 5 (b), MirrorFusion 2.0 delivers a convincing geometry with minimal artifacts, unlike the baseline, which fails to accurately capture the object’s geometry and appearance.

Qualitative results on the Real-World MSD dataset. MirrorFusion 2.0 performs well on MirrorBenchV2 and real-world objects from GSO but struggles with complex scenes, such as cluttered cables on a table and reflections across multiple mirrors (see Fig. 7). To improve coherence, we fine-tune it on a subset of the MSD dataset and

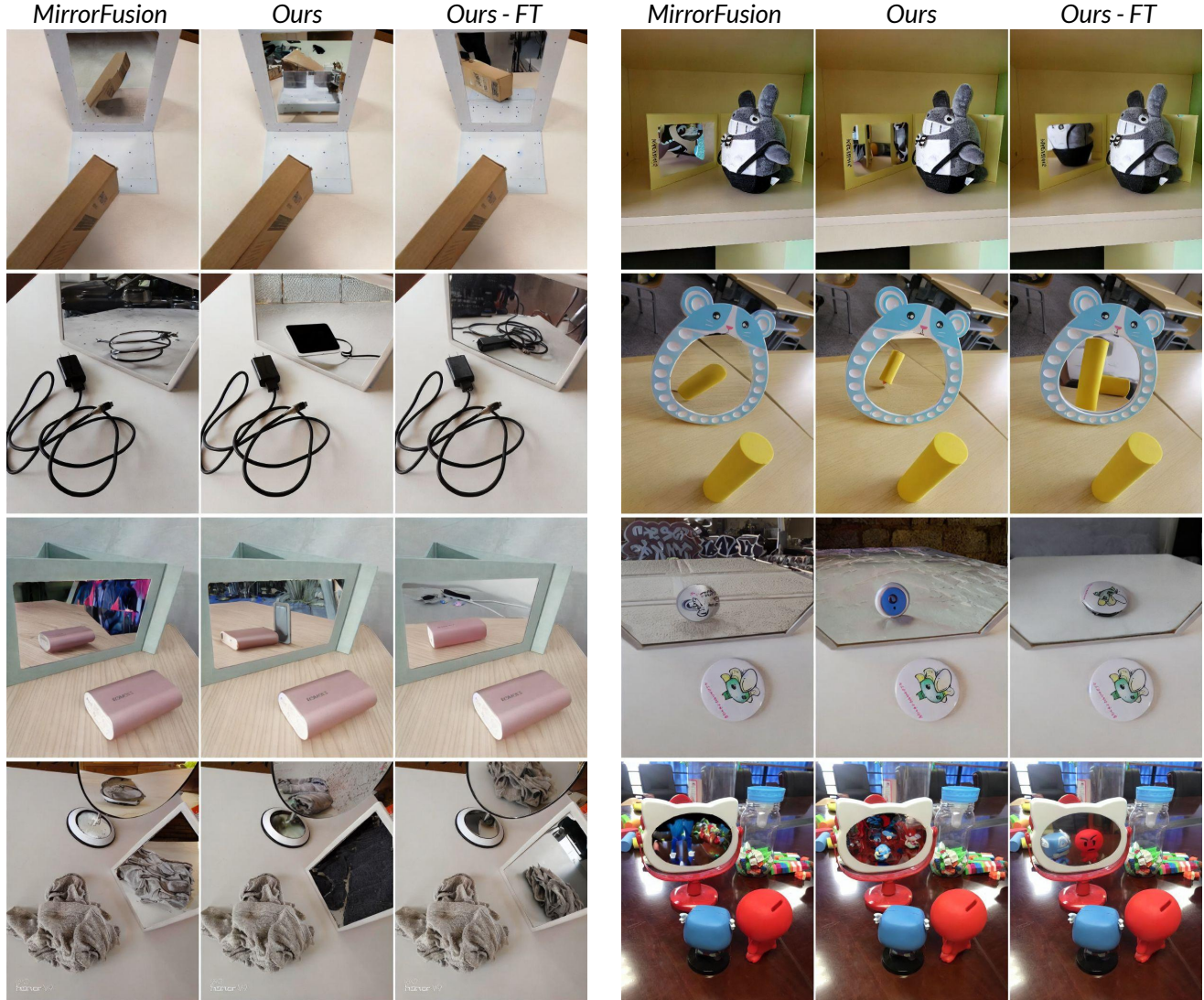


Figure 7. **Real World Scenes.** We show results for MirrorFusion [12], our method and our method fine-tuned on the MSD [52] dataset. We observe that our method can generate reflections capturing the intricacies of complex scenes, such as a cluttered cable on the table and the presence of two mirrors in a 3D scene.

test it on a held-out split, enhancing its ability to handle real-world scenarios. As shown in Fig. 7, this fine-tuning enables high-fidelity reflections, accurately capturing details like the “black cable” on the table and the “towel” in both mirrors. These results demonstrate how our dataset improves diffusion models, enabling more realistic reflections in challenging settings. Fig. 7 illustrates further examples on the real-world MSD dataset.

Quantitative results with baselines. For evaluating the metrics, we generate images using four seeds for a particular prompt and select the image that has the best SSIM score on the unmasked region. For a particular metric, we report the average value across MirrorBenchV2 by averaging the metric for all the selected images. Tabs. 2 and 3 show that



Table 2. **Single Object Reflection Generation Quality.** We compare the quantitative results between the baseline and MirrorFusion 2.0 on the **single object** split of MirrorBenchV2. The best results are shown in **bold**. This shows the effectiveness of the dataset by achieving improved scores.

| Metrics | Reflection Generation Quality | | | Text Alignment |
|----------------------|-------------------------------|-----------------|--------------------|---------------------|
| Models | PSNR \uparrow | SSIM \uparrow | LPIPS \downarrow | CLIP Sim \uparrow |
| baseline [12] | 18.31 | 0.76 | 0.122 | 26.00 |
| Ours 40k | 18.79 | 0.77 | 0.108 | 25.96 |

our method outperforms the baseline method and finetuning on multiple objects improves the results on complex scenes.

Table 3. **Multiple Object Reflection Generation Quality.** We compare the quantitative results between MirrorFusion 2.0 trained without multiple objects and MirrorFusion 2.0 trained with multiple objects on the **multiple object** split of MirrorBenchV2. The best results are shown in **bold**. This shows the effectiveness of finetuning further on multiple objects.

| Metrics | Reflection Generation Quality | | | Text Alignment |
|-----------------|-------------------------------|-----------------|--------------------|---------------------|
| Models | PSNR \uparrow | SSIM \uparrow | LPIPS \downarrow | CLIP Sim \uparrow |
| Ours 40k | 17.77 | 0.743 | 0.126 | 26.17 |
| Ours 50k | 18.00 | 0.744 | 0.119 | 26.09 |

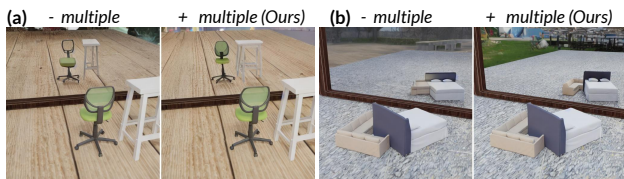


Figure 8. **Impact of adding multiple objects.** We observe that training without multiple objects leads to (a) poor reflection generation and (b) artifacts like object blending, supporting the need for finetuning the model on such scenarios.

User study. To evaluate the effectiveness of our proposed strategy, we also conducted a user study where we provided users with 40 different samples containing single, multiple, GSO objects, and real-world generations from the baseline and MirrorFusion 2.0. **84% of users preferred generations from MirrorFusion 2.0 over the baseline method.** We provide more details in Appendix D.5.

Limitations. Fig. 10 illustrates examples where our method accurately captures overall geometry but introduces minor artifacts which can be easily addressed by synthesizing additional training data and fine-tuning the model.

5.1. Ablation Studies

Impact of multiple objects dataset. To evaluate the impact of adding multiple objects to our dataset, we compare MirrorFusion 2.0 with (“+ multiple”) and without (“- multiple”) object training in Fig. 8. “MirrorFusion 2.0-w/o multiple” struggles to generate plausible mirror reflections, as evident in Fig. 8 (b), where the bed and sofa appear to blend together. In contrast, “MirrorFusion 2.0-with multiple” accurately captures the spatial relationships between objects within the mirror reflection. These results highlight the importance of including multiple objects in the dataset, enabling the model to learn spatial relationships and effectively handle occlusions.

Ablation on architecture. To further validate our architectural choice, we adapt Stable Diffusion Inpainting to accept depth maps as input similar to the changes made for MirrorFusion 2.0 and train this modified model on our pro-

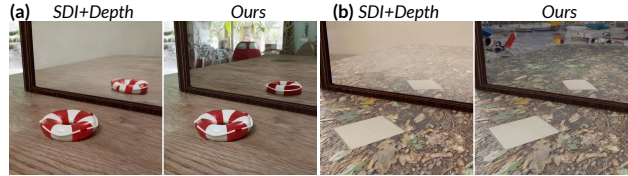


Figure 9. **Comparison with SDI+Depth baseline.** We observe color leakage issues in “SDI+Depth” generations. A dual-branch architecture proves to be a better choice, yielding superior outcomes.



Figure 10. **Limitations.** Our method performs well in multi-object scenes (more than two objects) but retains some artifacts, which can be reduced by synthesizing the dataset through the proposed data-generation pipeline and further increasing the diversity and scale.

posed dataset referring to it as “SDI+Depth”. We compare “SDI+Depth” with MirrorFusion 2.0 in Fig. 9. While “SDI+Depth” accurately positions objects in the mirror, it suffers from significant artifacts, including color leakage in contrast to MirrorFusion 2.0. We suspect that this happens due to the early combination of the noisy latent features, mask, and conditioning information in the initial convolution layer, restricting later layers from accessing clean features. These findings suggest that a dual branch architecture to provide the conditioning information separately as done in MirrorFusion 2.0 is a better choice.

6. Conclusion

We introduce SynMirrorV2, a novel large-scale synthetic dataset designed to advance mirror reflection generation significantly. By employing targeted data augmentations, we achieved robust variability in object pose, position, and occlusion, alongside the ability to handle multi-object scenes. Our qualitative and quantitative evaluations demonstrate SynMirrorV2’s efficacy in reflection generation, with promising generalization to real-world scenes using curriculum training. This dataset holds substantial potential for driving progress in various mirror-related tasks. Future research will explore advanced data augmentation techniques to enhance real-world performance further.

Acknowledgment. We are grateful to the Kotak IISc AI-ML Center for providing the computing resources. We thank Rishubh Parihar for their valuable feedback and Lokesh R. Boregowda for their valuable guidance.

References

- [1] Adobe. Adobe firefly. <https://www.adobe.com/products/firefly.html>, 2025. Accessed: 2025-03-23. 19, 20
- [2] Stability AI. Stable diffusion 3.5. <https://huggingface.co/stabilityai/stable-diffusion-3.5-large>, 2025. Accessed: 2025-03-23. 2, 3
- [3] Omri Avrahami, Dani Lischinski, and Ohad Fried. Blended diffusion for text-driven editing of natural images. In *Proceedings of the IEEE/CVF conference on computer vision and pattern recognition*, pages 18208–18218, 2022. 3
- [4] Omri Avrahami, Ohad Fried, and Dani Lischinski. Blended latent diffusion. *ACM transactions on graphics (TOG)*, 42(4):1–11, 2023. 3
- [5] Aleksei Bochkovskii, Amaël Delaunoy, Hugo Germain, Marcel Santos, Yichao Zhou, Stephan R. Richter, and Vladlen Koltun. Depth pro: Sharp monocular metric depth in less than a second. *arXiv preprint arXiv: 2410.02073*, 2024. 5
- [6] Jasmine Collins, Shubham Goel, Kenan Deng, Achleshwar Luthra, Leon Xu, Erhan Gundogdu, Xi Zhang, Tomas F Yago Vicente, Thomas Dideriksen, Himanshu Arora, et al. Abo: Dataset and benchmarks for real-world 3d object understanding. In *Proceedings of the IEEE/CVF conference on computer vision and pattern recognition*, pages 21126–21136, 2022. 3, 4
- [7] Katherine Crowson, Stefan Andreas Baumann, Alex Birch, Tanishq Mathew Abraham, Daniel Z Kaplan, and Enrico Shippole. Scalable high-resolution pixel-space image synthesis with hourglass diffusion transformers. In *Forty-first International Conference on Machine Learning*, 2024. 3
- [8] Giannis Daras, Mauricio Delbracio, Hossein Talebi, Alexandros G. Dimakis, and Peyman Milanfar. Soft diffusion: Score matching with general corruptions. *Trans. Mach. Learn. Res.*, 2023, 2023. 3
- [9] Matt Deitke, Dustin Schwenk, Jordi Salvador, Luca Weihs, Oscar Michel, Eli VanderBilt, Ludwig Schmidt, Kiana Ehsani, Aniruddha Kembhavi, and Ali Farhadi. Objaverse: A universe of annotated 3d objects. In *Proceedings of the IEEE/CVF Conference on Computer Vision and Pattern Recognition*, pages 13142–13153, 2023. 3
- [10] Maximilian Denninger, Dominik Winkelbauer, Martin Sundermeyer, Wout Boerdijk, Markus Wendelin Knauer, Klaus H Strobl, Matthias Humt, and Rudolph Triebel. Blenderproc2: A procedural pipeline for photorealistic rendering. *Journal of Open Source Software*, 8(82):4901, 2023. 3, 4
- [11] Prafulla Dhariwal and Alexander Nichol. Diffusion models beat gans on image synthesis. *Advances in neural information processing systems*, 34:8780–8794, 2021. 3
- [12] Ankit Dhiman, Manan Shah, Rishubh Parihar, Yash Bhalgat, Lokesh R Boregowda, and R Venkatesh Babu. Reflecting reality: Enabling diffusion models to produce faithful mirror reflections, 2024. 2, 3, 4, 5, 6, 7, 13
- [13] Laura Downs, Anthony Francis, Nate Koenig, Brandon Kinman, Ryan Hickman, Krista Reymann, Thomas B McHugh, and Vincent Vanhoucke. Google scanned objects: A high-quality dataset of 3d scanned household items. In *2022 International Conference on Robotics and Automation (ICRA)*, pages 2553–2560. IEEE, 2022. 5, 6, 19
- [14] Patrick Esser, Robin Rombach, and Bjorn Ommer. Taming transformers for high-resolution image synthesis. In *Proceedings of the IEEE/CVF conference on computer vision and pattern recognition*, pages 12873–12883, 2021. 2
- [15] Mark Edward M. Gonzales, Lorene C. Uy, and Joel P. Ila. Designing a lightweight edge-guided convolutional neural network for segmenting mirrors and reflective surfaces. *Computer Science Research Notes*, 3301:107–116, 2023. 2
- [16] Poly Haven. Poly haven : The public 3d asset library, 2025. Accessed: 2025-03-23. 3
- [17] Jonathan Ho, Ajay Jain, and Pieter Abbeel. Denoising diffusion probabilistic models. *Advances in neural information processing systems*, 33:6840–6851, 2020. 2, 3
- [18] Jonathan Ho, Tim Salimans, Alexey Gritsenko, William Chan, Mohammad Norouzi, and David J Fleet. Video diffusion models. *Advances in Neural Information Processing Systems*, 35:8633–8646, 2022. 2
- [19] Yicong Hong, Kai Zhang, Jiuxiang Gu, Sai Bi, Yang Zhou, Difan Liu, Feng Liu, Kalyan Sunkavalli, Trung Bui, and Hao Tan. Lrm: Large reconstruction model for single image to 3d. *ArXiv*, abs/2311.04400, 2023. 3
- [20] Xu Ju, Xian Liu, Xintao Wang, Yuxuan Bian, Ying Shan, and Qiang Xu. Brushnet: A plug-and-play image inpainting model with decomposed dual-branch diffusion. In *European Conference on Computer Vision*, 2024. 3, 4
- [21] Kunal Kathare, Ankit Dhiman, K Vikas Gowda, Siddharth Aravindan, Shubham Monga, Basavaraja Shanthappa Vandrotti, and Lokesh R Boregowda. Instructive3d: Editing large reconstruction models with text instructions. In *Proceedings of the Winter Conference on Applications of Computer Vision (WACV)*, pages 3246–3256, 2025. 3
- [22] Black Forest Labs. Flux. <https://github.com/black-forest-labs/flux>, 2025. Accessed: 2025-03-23. 2, 3
- [23] Zhimin Li, Jianwei Zhang, Qin Lin, Jiangfeng Xiong, Yanxin Long, Xincheng Deng, Yingfang Zhang, Xingchao Liu, Minbin Huang, Zedong Xiao, Dayou Chen, Jiajun He, Jiahao Li, Wenyue Li, Chen Zhang, Rongwei Quan, Jianxiang Lu, Jiabin Huang, Xiaoyan Yuan, Xiaoxiao Zheng, Yixuan Li, Jihong Zhang, Chao Zhang, Meng Chen, Jie Liu, Zheng Fang, Weiyan Wang, Jinbao Xue, Yangyu Tao, Jianchen Zhu, Kai Liu, Sihuan Lin, Yifu Sun, Yun Li, Dongdong Wang, Mingtao Chen, Zhichao Hu, Xiao Xiao, Yan Chen, Yuhong Liu, Wei Liu, Di Wang, Yong Yang, Jie Jiang, and Qinglin Lu. Hunyuan-dit: A powerful multi-resolution diffusion transformer with fine-grained chinese understanding, 2024. 2
- [24] Jiaying Lin, Guodong Wang, and Rynson W.H. Lau. Progressive mirror detection. In *Proc. CVPR*, 2020. 2
- [25] Ilya Loshchilov and Frank Hutter. Decoupled weight decay regularization. In *International Conference on Learning Representations*, 2017. 5
- [26] Andreas Lugmayr, Martin Danelljan, Andres Romero, Fisher Yu, Radu Timofte, and Luc Van Gool. Repaint: Inpainting

- using denoising diffusion probabilistic models. In *Proceedings of the IEEE/CVF conference on computer vision and pattern recognition*, pages 11461–11471, 2022. 3
- [27] Hayk Manukyan, Andranik Sargsyan, Barsegh Atanyan, Zhangyang Wang, Shant Navasardyan, and Humphrey Shi. Hd-painter: high-resolution and prompt-faithful text-guided image inpainting with diffusion models. *arXiv preprint arXiv:2312.14091*, 2023. 2, 3
- [28] Haiyang Mei, Bo Dong, Wen Dong, Pieter Peers, Xin Yang, Qiang Zhang, and Xiaopeng Wei. Depth-aware mirror segmentation. In *Proceedings of the IEEE/CVF conference on computer vision and pattern recognition*, pages 3044–3053, 2021. 2
- [29] Oscar Michel, Anand Bhattad, Eli VanderBilt, Ranjay Krishna, Aniruddha Kembhavi, and Tanmay Gupta. Object 3dit: Language-guided 3d-aware image editing. *Advances in Neural Information Processing Systems*, 36, 2024. 2, 3
- [30] Sicheng Mo, Fangzhou Mu, Kuan Heng Lin, Yanli Liu, Bochen Guan, Yin Li, and Bolei Zhou. Freecontrol: Training-free spatial control of any text-to-image diffusion model with any condition. In *Proceedings of the IEEE/CVF Conference on Computer Vision and Pattern Recognition*, pages 7465–7475, 2024. 2
- [31] Rishubh Parihar, Abhijnya Bhat, Abhipsa Basu, Saswat Mallick, Jogendra Nath Kundu, and R Venkatesh Babu. Balancing act: distribution-guided debiasing in diffusion models. In *Proceedings of the IEEE/CVF conference on computer vision and pattern recognition*, pages 6668–6678, 2024. 3
- [32] Rishubh Parihar, Harsh Gupta, Sachidanand VS, and R Venkatesh Babu. Text2place: Affordance-aware text guided human placement. In *European Conference on Computer Vision*, pages 57–77. Springer, 2024. 3
- [33] Rishubh Parihar, VS Sachidanand, Sabariswaran Mani, Tejan Karmali, and R Venkatesh Babu. Precisecontrol: Enhancing text-to-image diffusion models with fine-grained attribute control. In *European Conference on Computer Vision*, pages 469–487. Springer, 2024. 3
- [34] William Peebles and Saining Xie. Scalable diffusion models with transformers. In *Proceedings of the IEEE/CVF International Conference on Computer Vision*, pages 4195–4205, 2023. 3
- [35] Dustin Podell, Zion English, Kyle Lacey, Andreas Blattmann, Tim Dockhorn, Jonas Müller, Joe Penna, and Robin Rombach. Sdxl: Improving latent diffusion models for high-resolution image synthesis. *arXiv preprint arXiv:2307.01952*, 2023. 2
- [36] Alec Radford, Jong Wook Kim, Chris Hallacy, Aditya Ramesh, Gabriel Goh, Sandhini Agarwal, Girish Sastry, Amanda Askell, Pamela Mishkin, Jack Clark, et al. Learning transferable visual models from natural language supervision. In *International conference on machine learning*, pages 8748–8763. PMLR, 2021. 6
- [37] Aditya Ramesh, Prafulla Dhariwal, Alex Nichol, Casey Chu, and Mark Chen. Hierarchical text-conditional image generation with clip latents. *arXiv preprint arXiv:2204.06125*, 1(2):3, 2022. 3
- [38] Robin Rombach, Andreas Blattmann, Dominik Lorenz, Patrick Esser, and Björn Ommer. High-resolution image synthesis with latent diffusion models. In *Proceedings of the IEEE/CVF conference on computer vision and pattern recognition*, pages 10684–10695, 2022. 2, 3
- [39] Chitwan Saharia, William Chan, Huiwen Chang, Chris Lee, Jonathan Ho, Tim Salimans, David Fleet, and Mohammad Norouzi. Palette: Image-to-image diffusion models. In *ACM SIGGRAPH 2022 conference proceedings*, pages 1–10, 2022. 3
- [40] Chitwan Saharia, William Chan, Saurabh Saxena, Lala Li, Jay Whang, Emily L Denton, Kamyar Ghasemipour, Raphael Gontijo Lopes, Burcu Karagol Ayan, Tim Salimans, et al. Photorealistic text-to-image diffusion models with deep language understanding. *Advances in neural information processing systems*, 35:36479–36494, 2022. 3
- [41] Ayush Sarkar, Hanlin Mai, Amitabh Mahapatra, Svetlana Lazebnik, David A Forsyth, and Anand Bhattad. Shadows don’t lie and lines can’t bend! generative models don’t know projective geometry... for now. In *Proceedings of the IEEE/CVF Conference on Computer Vision and Pattern Recognition*, pages 28140–28149, 2024. 2, 3
- [42] Prafull Sharma, Varun Jampani, Yuanzhen Li, Xuhui Jia, Dmitry Lagun, Fredo Durand, Bill Freeman, and Mark Matthews. Alchemist: Parametric control of material properties with diffusion models. In *Proceedings of the IEEE/CVF Conference on Computer Vision and Pattern Recognition*, pages 24130–24141, 2024. 3
- [43] Jascha Sohl-Dickstein, Eric Weiss, Niru Maheswaranathan, and Surya Ganguli. Deep unsupervised learning using nonequilibrium thermodynamics. In *International conference on machine learning*, pages 2256–2265. PMLR, 2015. 3
- [44] Tianyu Sun, Guodong Zhang, Wenming Yang, Jing-Hao Xue, and Guijin Wang. Trosd: A new rgb-d dataset for transparent and reflective object segmentation in practice. *IEEE Transactions on Circuits and Systems for Video Technology*, 33(10):5721–5733, 2023. 2
- [45] Jiaqi Tan, Weijie Lin, Angel X Chang, and Manolis Savva. Mirror3D: Depth refinement for mirror surfaces. In *Proceedings of the IEEE Conference on Computer Vision and Pattern Recognition (CVPR)*, 2021. 2
- [46] Rishi Upadhyay, Howard Zhang, Yunhao Ba, Ethan Yang, Blake Gella, Sicheng Jiang, Alex Wong, and Achuta Kadambi. Enhancing diffusion models with 3d perspective geometry constraints. *ACM Transactions on Graphics (TOG)*, 42(6):1–15, 2023. 2, 3
- [47] A Vaswani. Attention is all you need. *Advances in Neural Information Processing Systems*, 2017. 3
- [48] Bram Wallace, Akash Gokul, and Nikhil Naik. Edict: Exact diffusion inversion via coupled transformations. In *Proceedings of the IEEE/CVF Conference on Computer Vision and Pattern Recognition*, pages 22532–22541, 2023. 3
- [49] Daniel Winter, Matan Cohen, Shlomi Fruchter, Yael Pritch, Alex Rav-Acha, and Yedid Hoshen. Objectdrop: Bootstrapping counterfactuals for photorealistic object removal and insertion, 2024. 2, 3

- [50] Xiaojun Wu, Dixiang Zhang, Ruyi Gan, Junyu Lu, Ziwei Wu, Renliang Sun, Jiaying Zhang, Pingjian Zhang, and Yan Song. Taiyi-diffusion-xl: Advancing bilingual text-to-image generation with large vision-language model support, 2024. [2](#)
- [51] Shaoan Xie, Zhifei Zhang, Zhe Lin, Tobias Hinz, and Kun Zhang. Smartbrush: Text and shape guided object inpainting with diffusion model. In *Proceedings of the IEEE/CVF Conference on Computer Vision and Pattern Recognition*, pages 22428–22437, 2023. [3](#)
- [52] Xin Yang, Haiyang Mei, Ke Xu, Xiaopeng Wei, Baocai Yin, and Rynson W.H. Lau. Where is my mirror? In *The IEEE International Conference on Computer Vision (ICCV)*, 2019. [2](#), [5](#), [7](#), [19](#), [20](#)
- [53] Fulong Ye, Guangyi Liu, Xinya Wu, and Ledell Yu Wu. Alt-diffusion: A multilingual text-to-image diffusion model. In *AAAI Conference on Artificial Intelligence*, 2023. [2](#)
- [54] Hu Ye, Jun Zhang, Sibao Liu, Xiao Han, and Wei Yang. Ip-adapter: Text compatible image prompt adapter for text-to-image diffusion models. *arXiv preprint arXiv:2308.06721*, 2023. [2](#)
- [55] Junyi Zeng, Chong Bao, Rui Chen, Zilong Dong, Guofeng Zhang, Hujun Bao, and Zhaopeng Cui. Mirror-nerf: Learning neural radiance fields for mirrors with whitted-style ray tracing. In *Proceedings of the 31st ACM International Conference on Multimedia*, pages 4606–4615, 2023. [2](#)
- [56] Lvmin Zhang, Anyi Rao, and Maneesh Agrawala. Adding conditional control to text-to-image diffusion models. In *Proceedings of the IEEE/CVF International Conference on Computer Vision*, pages 3836–3847, 2023. [2](#)
- [57] Richard Zhang, Phillip Isola, Alexei A Efros, Eli Shechtman, and Oliver Wang. The unreasonable effectiveness of deep features as a perceptual metric. In *Proceedings of the IEEE conference on computer vision and pattern recognition*, pages 586–595, 2018. [5](#)
- [58] Shihao Zhao, Dongdong Chen, Yen-Chun Chen, Jianmin Bao, Shaozhe Hao, Lu Yuan, and Kwan-Yee K Wong. Uni-controlnet: All-in-one control to text-to-image diffusion models. *Advances in Neural Information Processing Systems*, 36, 2024. [2](#)
- [59] Wenliang Zhao, Lujia Bai, Yongming Rao, Jie Zhou, and Jiwen Lu. Unipc: A unified predictor-corrector framework for fast sampling of diffusion models. *Advances in Neural Information Processing Systems*, 36, 2024. [5](#)
- [60] Hongkai Zheng, Weili Nie, Arash Vahdat, and Anima Anandkumar. Fast training of diffusion models with masked transformers. *Trans. Mach. Learn. Res.*, 2024, 2023. [3](#)
- [61] Junhao Zhuang, Yanhong Zeng, Wenran Liu, Chun Yuan, and Kai Chen. A task is worth one word: Learning with task prompts for high-quality versatile image inpainting. In *European Conference on Computer Vision*, 2023. [3](#)

MirrorVerse: Pushing Diffusion Models to Realistically Reflect the World

Supplementary Material

Contents

| | |
|--|-----------|
| A Dataset Generation | 12 |
| B Architecture Details | 13 |
| C Additional Details | 16 |
| C.1. Characteristic Comparison with SynMirror | 16 |
| C.2. Text prompts used in the experiments | 16 |
| D Additional Results | 17 |
| D.1. Affect of Joint training with single and multiple objects | 17 |
| D.2. Additional results from single object scenes from MirrorBenchV2 | 17 |
| D.3. Additional results from multiple object scenes from MirrorBenchV2 | 17 |
| D.4. Comparison by fine-tuning only on the MSD dataset | 18 |
| D.5. User Study Details | 19 |
| D.6. Comparison with Commercial Product | 19 |

A. Dataset Generation

Grounding Object. We describe the algorithm to ground an object in Algorithm 2. If the minimum value of the bounding box along the z-dimension is greater than the ground level, we adjust the object’s position to rest it on the ground. This adjustment enhances the photorealism of the generated dataset, ensuring objects appear naturally grounded in their environment.

Sampling Region For random positions in front of the mirror, we first define a region in the x-y plane where the object and its reflection are visible in the camera view. To determine this region, we compute the intersection of the camera’s viewing frustum on the x-y plane with the extent of the mirror. This process is repeated for all camera locations used in the dataset generation. The resulting sampling region, \mathcal{S} , ensures that any position within it allows the visibility of both the object and its reflection in the camera view.

Object Placement We provide the procedure to place an object in a scene in Algorithm 3. First, we scale an object to fit inside a unit cube, ensuring uniformity across objects. Next, we randomly sample a position in front of the mirror and update the position of the object accordingly. Finally,

Algorithm 2 Procedure to Ground an Object

Require: Input 3D model \mathcal{M} , Ground-Level \underline{Z}

- 1: **Function** GROUNDOBJECT($\mathcal{M}, \underline{Z}$)
- 2: $bbox \leftarrow \text{GETBOUNDINGBOX3D}(\mathcal{M})$
- 3: **if** $bbox.z > \underline{Z}$ **then**
- 4: $z \leftarrow bbox.z - \underline{Z}$
- 5: $\Delta t \leftarrow [0, 0, -z]$
- 6: $\mathcal{M}.position \leftarrow \mathcal{M}.position + \Delta t$
- 7: **end if**

Algorithm 3 Procedure to Place an Object in a scene

Require: Input 3D model \mathcal{M} , Ground-Level \underline{Z} , Sampling region \mathcal{S}

- 1: **Function** NORMALIZEOBJECT(\mathcal{M})
- 2: $bbox \leftarrow \text{GETBOUNDINGBOX3D}(\mathcal{M})$
- 3: $d_{max} \leftarrow \text{GetMaxDimension}(bbox)$
- 4: $s \leftarrow \frac{1}{d_{max}}$
- 5: $S_{matrix} \leftarrow \text{GetScaleMatrix}(s)$
- 6: $\mathcal{M}.scale \leftarrow S_{matrix}$
- 7: $bbox \leftarrow \text{GETBOUNDINGBOX3D}(\mathcal{M})$
- 8: **return** $bbox$
- 9:
- 10: **Function** SAMPLEPOSITION(\mathcal{M}, \mathcal{S})
- 11: $t \leftarrow \text{SamplePosition}(\mathcal{S})$
- 12: $\mathcal{M}.translation \leftarrow t$
- 13: $bbox \leftarrow \text{GETBOUNDINGBOX3D}(\mathcal{M})$
- 14: **return** $bbox$
- 15:
- 16: **Function** RANDOMROTATION(\mathcal{M})
- 17: $\theta \leftarrow \text{RandomAngle}(\mathcal{S})$
- 18: $R_{matrix} \leftarrow \text{GetRotationMatrix}(\theta)$
- 19: $\mathcal{M}.rotation \leftarrow R_{matrix}$
- 20: $bbox \leftarrow \text{GETBOUNDINGBOX3D}(\mathcal{M})$
- 21: **return** $bbox$
- 22:
- 23: **Main Algorithm**
- 24: $bbox \leftarrow \text{NORMALIZEOBJECT}(\mathcal{M})$
- 25: $bbox \leftarrow \text{SAMPLEPOSITION}(\mathcal{M}, \mathcal{S})$
- 26: $bbox \leftarrow \text{RANDOMROTATION}(\mathcal{M})$

we apply a random rotation around the vertical axis. These steps guarantee that the object and its reflection remain visible in the camera’s field of view. Further, these steps introduce greater diversity to the dataset.

Additional Samples. We provide additional samples for scenes with single object in Fig. 13 and multiple objects in

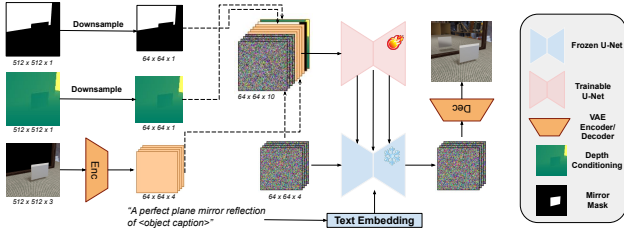


Figure 11. Overview of architecture used for the experiments.



Figure 12. Samples of scenes containing more than two objects.

Figs. 12 and 14. Further, we also provide additional samples for visualization from SynMirrorV2 in folder “dataset-samples” in the attached supplementary material.

B. Architecture Details

Our work builds upon the MirrorFusion framework [12], which employs a conditioning network that leverages depth information to guide the generation process of a pre-trained generative network. This model is trained using a three-stage curriculum learning strategy, as detailed in Sec. 4.



Figure 13. Samples of scene containing single object from SynMirrorV2



Figure 14. Samples of scene containing multiple objects from SynMirrorV2

Table 4. Comparison of the proposed dataset, SynMirrorV2 , with SynMirror

| Augmentations | Grounding | Random Rotations | Random Positions | Multiple Objects | Occlusion Scenarios |
|---------------|-----------|------------------|------------------|------------------|---------------------|
| SynMirror | ✗ | ✗ | ✗ | ✗ | ✗ |
| SynMirrorV2 | ✓ | ✓ | ✓ | ✓ | ✓ |

C. Additional Details

C.1. Characteristic Comparison with SynMirror

We present a characteristic comparison of the proposed dataset with SynMirror in Tab. 4. This variety aids in the generalization of the MirrorFusion 2.0 to complex scenarios and real-world scenes.

C.2. Text prompts used in the experiments

We provide the text prompts used in the main paper for image generation.

Figure 1. Each row in this figure uses the same text prompt. Text prompts are as follows:

- **First row.** “A perfect plane mirror reflection of (A cylindrical bottle with a spherical top and bottom, featuring a neck and spout.) and (A cylinder with a conical bottom and a spherical top.)”
- **Second row.** “A perfect plane mirror reflection of a yellow mug with a flower design is placed on a desk in front of a mirror. The reflection of the mug can be seen in the mirror, creating an interesting visual effect where the mug appears to be floating.”

Figure 4. Text prompts are as follows:

- (a) “A perfect plane mirror reflection of a chair with a high, rounded back and blue upholstery.”
- (b) “A perfect plane mirror reflection of (3D model of a Chesterfield sofa with cylindrical and spherical elements.) and (3D model of a two-seater sofa with backrest and armrests.)”

Figure 5. Text prompts are as follows:

- (a) “A perfect plane mirror reflection of a black color furniture in stair shape with multiple drawers.”
- (b) “A perfect plane mirror reflection of a yellow and white mug on a grey surface.”

Figure 6. Text prompts for “Column-1” are as follows:

- **First row.** “A perfect plane mirror reflection of a curved and slatted 3D chair with backrest, seat, armrests, and footrest.”
- **Second row.** “A perfect plane mirror reflection of a croissant that is chocolate and covered in nuts on one side and plain on the other.”

- **Third row.** “A perfect plane mirror reflection of (A wooden stool with a backrest and a seat.) and (3D model of a lamp with a cylindrical body, spherical base, conical bottom, spherical top, and a cylindrical shade with a spherical accent.)”

- **Fourth row.** “A perfect plane mirror reflection of (King size bed with a slatted base, tufted headboard and footboard, curved backrest and armrest, and slanted top and bottom edges.) and (A 3D object with a truncated octagonal base and a spherical top.)”

Text prompts for “Column-2” are as follows:

- **First row.** “A perfect plane mirror reflection of an orange vat sitting on a grey metal frame with a light gray colored control box attached.”
- **Second row.** “A perfect plane mirror reflection of a dark blue baby buggy with no one in it.”
- **Third row.** “A perfect plane mirror reflection of (A 3D model of a single-seater Chesterfield sofa with a tufted back, curved backrest, and slanted seat.) and (Rectangular cabinet with a slanted roof and base, featuring a door and a drawer, 3D modeled as a TV stand.)”
- **Fourth row.** “A perfect plane mirror reflection of (3D model of a kitchen cart with three shelves, two drawers on each side, and a two-tiered bunk bed with slatted bases.) and (Three-tiered wheeled cart with shelves and a handle.)”

Figure 7. Text prompts for “Column-1” are as follows:

- **First row.** “The dynamics of the mirror and its reflections involve the use of a cardboard box. The box is placed on top of a table, and the mirror is positioned in such a way that it reflects the surrounding environment.”
- **Second row.** “The mirror’s reflection in the cord creates an interesting visual effect, making it appear as if the cord is coming out of the mirror itself. This setup can be useful for individuals who need to charge their electronic devices while working.”
- **Third row.** “A pink portable charger is placed on a wooden table next to a mirror. The mirror reflects the portable charger, creating an interesting dynamic between the object and its reflection in the mirror.”
- **Fourth row.** “The mirror reflects a pile of dirty clothes or towels, which appear to be wrinkled and disheveled. This phenomenon is caused by the way light bounces off the surface of the mirror and interacts with the objects in front of it”

Text prompts for “Column-2” are as follows:

- **First row.** “Anamorphosis is a technique used to create distorted images that appear normal when viewed from a specific vantage point. In this case, the viewer needs to be positioned directly in front of the mirror to see the full effect of the toy”
- **Second row.** “A toy mouse-shaped mirror is placed on a

Table 5. Ablation studies on mixed-training for multiple objects

| Metrics | Reflection Generation Quality | | | Text Alignment |
|-----------------------|-------------------------------|-----------------|--------------------|---------------------|
| Models | PSNR \uparrow | SSIM \uparrow | LPIPS \downarrow | CLIP Sim \uparrow |
| Joint Training | 17.41 | 0.615 | 0.153 | 26.37 |
| Ours 50k | 18.00 | 0.744 | 0.119 | 26.09 |

table in front of a yellow cylindrical object. The mirror reflects the environment around it, including the yellow cylinder and other objects in the room.”

- **Third row.** “The mirror is reflecting a small button with a cartoon character on it, which is placed on a white surface. The reflection of the button in the mirror creates an interesting visual effect, as the character appears to be floating or hovering”
- **Fourth row.** “The mirror in the image is reflecting two toy figures, a red one and a blue one, as they interact with each other. This dynamic creates a playful and imaginative scene, as the toys appear to be having a conversation.”

Figure 8. Text prompts are as follows:

- **(a)** “A perfect plane mirror reflection of (A swivel chair with a mesh seat, backrest, and swivel base.) and (A wooden cuboid stool with a square base, slanted square seat, and slanted backrest.)”
- **(b)** “A perfect plane mirror reflection of (L-shaped sectional sofa with U-shaped backrest, 3D model.) and (A king size bed with a tufted headboard, footboard, slatted base, and a single seater sofa with a backrest and seat cushion.)”

Figure 9. Text prompts are as follows:

- **(a)** “A perfect plane mirror reflection of a red and white striped round life buoy surrounded in a cord.”
- **(b)** “A perfect plane mirror reflection of a rug”

D. Additional Results

D.1. Affect of Joint training with single and multiple objects

An ablation study in Tab. 5 reveals the significant impact of staged training on generalization. Training on single and multiple splits simultaneously yielded inferior results, highlighting the importance of our staged approach. Curriculum training further allows us to fine-tune on real-world data such as the MSD dataset, providing better results than direct single-stage training as shown in Appendix D.4 and Fig. 16.

D.2. Additional results from single object scenes from MirrorBenchV2

We present additional results for single objects in Fig. 15. Observe that the baseline method produces several inaccuracies: the object (**Column 1, Row 2**) appears to be floating in mid-air with incorrect orientation, and the bullets (**Column 2, Row 2**) are also misaligned. Additionally, the reflection of the wooden table (**Column 1, Row 5**) has distorted legs. In contrast, our results accurately capture the geometry and appearance of the object in its reflection.

Text prompts for “**Column-1**” in Fig. 15 are as follows:

- **First row.** “A perfect plane mirror reflection of a shiny dark wooden pepper mill, stood upright, with a silver ornament on the top.”
- **Second row.** “A perfect plane mirror reflection of a white gravy boat with designs of pink flowers on the side and front with green foliage.”
- **Third row.** “A perfect plane mirror reflection of an orange and black two wheeled hoverboard.”
- **Fourth row.** “A perfect plane mirror reflection of a 3D swivel chair model with a curved backrest, armrests, and a swivel base.”
- **Fifth row.** “A perfect plane mirror reflection of a swivel chair with a slender, curved backrest and armrests, featuring a slanted seat.”

Text prompts for “**Column-2**” in Fig. 15 are as follows:

- **First row.** “A perfect plane mirror reflection of a swivel chair with a slender, curved backrest and armrests, featuring a slanted seat.”
- **Second row.** “A perfect plane mirror reflection of two metal bullets for either a gun or cannon.”
- **Third row.** “A perfect plane mirror reflection of a two-seater sofa with curved backrest, slanted seat, and armrests.”
- **Fourth row.** “A perfect plane mirror reflection of a 3D lamp with a cylindrical metal arm, spherical metal base, and spherical glass shade.”
- **Fifth row.** “A perfect plane mirror reflection of a rectangular table with a slatted, slanted top, hairpin legs, and a metal frame.”

D.3. Additional results from multiple object scenes from MirrorBenchV2

We present additional results for multiple objects in Fig. 19. The baseline method struggles to generate accurate reflections in scenes with multiple objects compared to its performance in single-object scenes. Notably, reflections of two sofas (**Column 1, Row 4**) and a sofa-table (**Column 2, Row 4**) pair are incorrectly merged, and in some cases, only a single object is rendered in the reflection. This poor performance is primarily due to the limited diversity of the dataset used to train the baseline method. In contrast, our approach preserves the original geometry of the objects, accurately

captures their spatial relationships, and maintains their appearance, resulting in significantly more realistic and consistent reflections for scenes with multiple objects.

Text prompts for “**Column-1**” in Fig. 19 are as follows:

- **First row.** “A perfect plane mirror reflection of a (rug) and (Rectangular cabinet with a slanted roof and base, featuring a door and a drawer, 3D modeled as a TV stand.)”
- **Second row.** “A perfect plane mirror reflection of a (3D model of a chair with a backrest, armrests, and seat.) and (Spherical table with a round top, square slanted base, and two slender legs.)”
- **Third row.** “A perfect plane mirror reflection of (A 3D model of a chair with a curved, tufted backrest, padded seat, armrests, and a squarish bowl with a matching base and lid.) and (rug).”
- **Fourth row.** “A perfect plane mirror reflection of (A 3D model of a two to three-seater sofa with a curved, tufted backrest, armrests, and a footrest.) and (3D model of a three-seater sofa with a curved backrest and armrests.)”
- **Fifth row.** “A perfect plane mirror reflection of (Cylindrical stool with a spherical top, square base, slanted seat, and backrest.) and (A cuboid with a base, spherical lid, and slanted top and bottom.)”
- **Sixth row.** “A perfect plane mirror reflection of (A cylinder with a spherical base and a spherical shade.) and (3D object: Slatted swivel chair with a curved, slanted X-shaped backrest and seat, featuring armrests and legs.)”
- **Seventh row.** “A perfect plane mirror reflection of (3D model of a chaise lounge featuring a curved backrest, cushioned seat, armrests, and footrest, made from a single piece of foam.) and (A 3D object resembling a book with a convex spine, slanted top and bottom edges, and stacked pages.)”
- **Eighth row.** “A perfect plane mirror reflection of (Two-seater couch with backrest and armrests, and a tetrahedral box with lid.) and (3D model of a rectangular coffee table with a slanted shelf on top, supported by a slanted frame.)”

Text prompts for “**Column-2**” in Fig. 19 are as follows:

- **First row.** “A perfect plane mirror reflection of (3D model of stacked cylindrical objects with spherical tops, resembling trash cans or water cisterns, featuring a tetrahedral cuboid and a truncated octahedral.) and (Three-drawer dresser with a slanted top, rectangular base, and rectilinear design.)”
- **Second row.** “A perfect plane mirror reflection of a (3D model of a chair with a backrest, armrests, and seat.) and (Spherical table with a round top, square slanted base, and two slender legs.)”
- **Third row.** “A perfect plane mirror reflection of (rug) and (3D model of a slanted rectangular coffee table in 3ds Max, available for download.)”

- **Fourth row.** “A perfect plane mirror reflection of (Three-seater grey sofa with a curved backrest and armrests in 3D.) and (A 3D tetrahedral desk with a slanted top, two drawers, a shelf, and a truncated triangular base.)”
- **Fifth row.** “A perfect plane mirror reflection of (A 3D model of a rectangular table with a pair of legs and a top.) and (Two-seater sofa with curved backrest and armrests, 3D model.)”
- **Sixth row.** “A perfect plane mirror reflection of (Swivel bar stool with a cylindrical seat, curved backrest, and swivel functionality.) and (Tall cabinet with a triangular base, slanted roof, flat top, and a retractable banner stand.)”
- **Seventh row.** “A perfect plane mirror reflection of (A wooden stool with a backrest and a seat.) and (3D model of a lamp with a cylindrical body, spherical base, conical bottom, spherical top, and a cylindrical shade with a spherical accent.)”
- **Eighth row.** “A perfect plane mirror reflection of (A king-size platform bed with a box-shaped, curved-top headboard, footboard, side rails, slatted base, and curved backrest.) and (U-shaped sectional sofa with multiple L-shaped sections, featuring backrests and armrests.)”

D.4. Comparison by fine-tuning only on the MSD dataset

To highlight the impact of the proposed dataset SynMirrorV2 and stage-wise training more profoundly, we compare our model (which is trained in 3 stages with the first two involving SynMirrorV2) with the model only finetuned directly on the MSD dataset for 10k iterations (i.e only stage 3) from the Stable Diffusion v1.5 checkpoint. We call the fine-tuned model “MSD-10k-FT”. We compare “MSD-10k-FT” with results from our method in Fig. 16. Note the orientation of the power bank is incorrect (**Second Row**), a brown toy is not generated in the reflection (**Third Row**) and a pink cup is generated instead of the white teapot (**Fourth Row**) in the results from “MSD-10k-FT”. This shows the importance of the proposed synthetic dataset for incorporating the priors of accurate mirror reflections and the importance of stage-wise finetuning to bridge the generalization gap.

Text prompts used in Fig. 16 are as follows:

- **First row.** “A perfect plane mirror reflection of a cardboard box placed on top of a table”
- **Second row.** “A perfect plane mirror reflection of a pink portable charger is placed on a wooden table.”
- **Third row.** “A perfect plane mirror reflection of a toy poop emoji figurine placed along with a blue cuboid and a green cylindrical object.”
- **Fourth row.** “A perfect plane mirror reflection of a pink and white ceramic mug with a smiling face on it.”

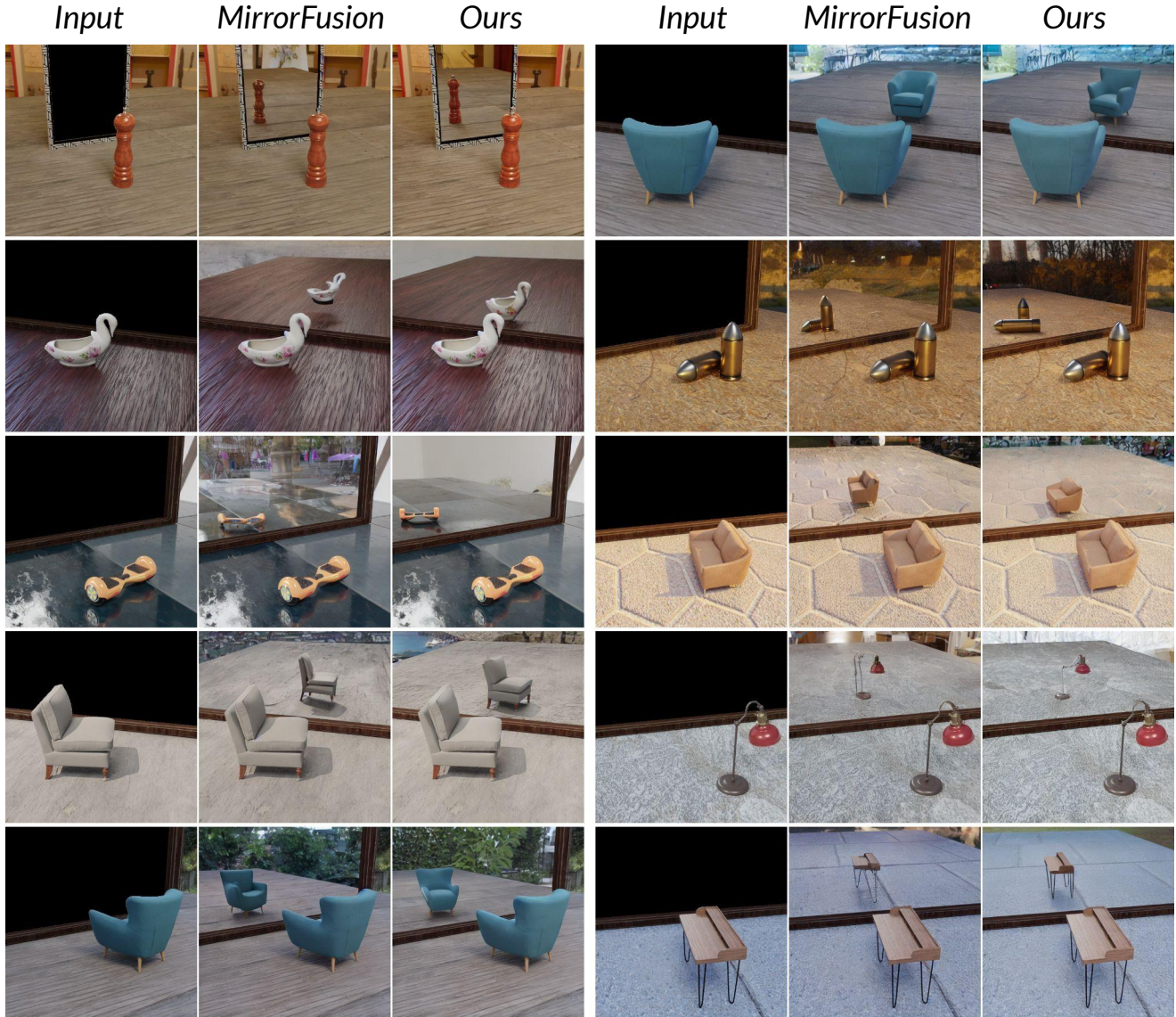


Figure 15. Results on scenes with single objects. More discussion in Appendix D.2.

D.5. User Study Details

We provide details of the user study described in Section 4 of the main paper. We selected 40 samples, including single-object and multi-object scenes, from MirrorBenchV2, GSO [13], and real-world scenes from MSD [52]. These samples were generated by the baseline method MirrorFusion and our method MirrorFusion 2.0.

We invited 29 participants (aged 18–50) to compare results based on the realism and plausibility of mirror reflections. Each task involved evaluating and selecting the best result among the outputs from both models with instructions to assess factors such as:

- Apparent distance and alignment of objects in the reflection.

tion.

- Geometry consistency and subtle details in reflections.
- Floor reflections and shadow orientations, if present.

Fig. 17 shows that our method was preferred in 84% of cases.

D.6. Comparison with Commercial Product

We compare our method with Adobe Firefly [1] in Fig. 18. Our method demonstrates superior performance compared to a widely used commercial product, Adobe Firefly, in generating accurate reflections on a mirror plane. Notably, the commercial product places reflections incorrectly for multiple objects in the scene (top row) and mispositions the reflection of the yellow mug (bottom row). Additionally, the

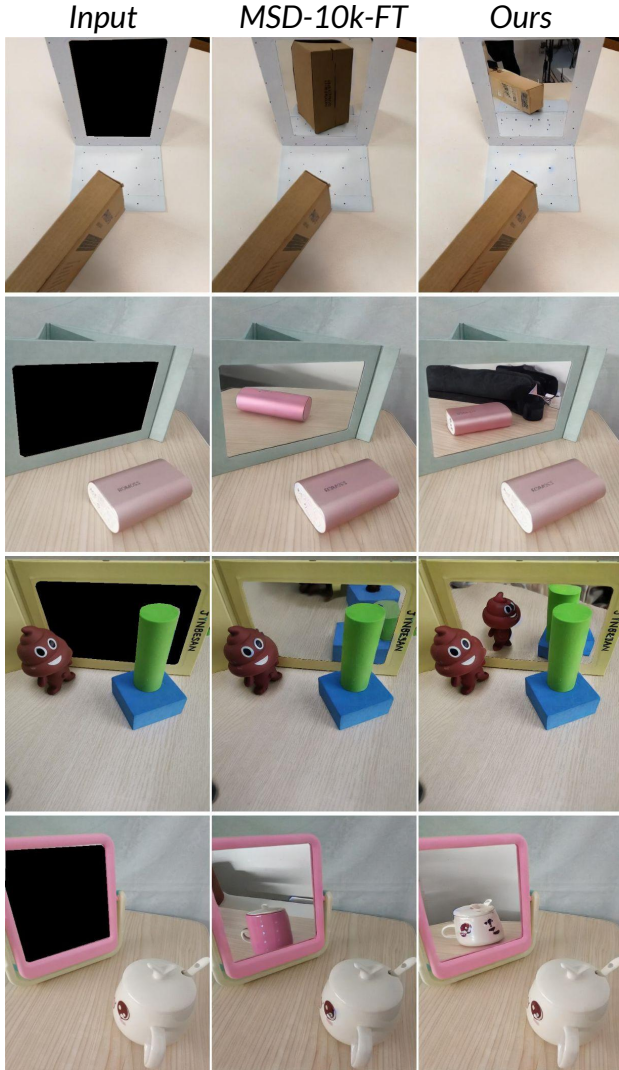


Figure 16. **Comparison with “MSD-10k-FT”**. We finetune our model directly on the MSD dataset [52] for 10k iterations and compare the results with our full 3-stage finetuning approach. More discussion in Appendix D.4.

orientation of objects in the inpainted region is inaccurate. In contrast, our method consistently generates reflections in the correct positions while preserving their proper orientation and appearance, resulting in more realistic and visually accurate outcomes. Text prompts used in Fig. 18 are as follows:

- **First row.** “A perfect plane mirror reflection of (A cylindrical bottle with a spherical top and bottom, featuring a neck and spout.) and (A cylinder with a conical bottom and a spherical top.)”
- **Second row.** “A perfect plane mirror reflection of a yellow mug with a flower design is placed on a desk in front of a mirror. The reflection of the mug can be seen in the

Inpainting User Study

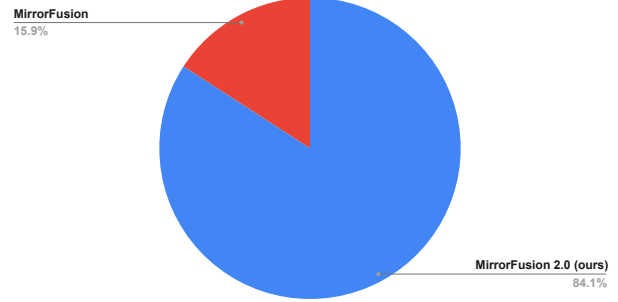


Figure 17. Visual comparison of outputs from our method and the baseline. We discuss in detail in Appendix D.5

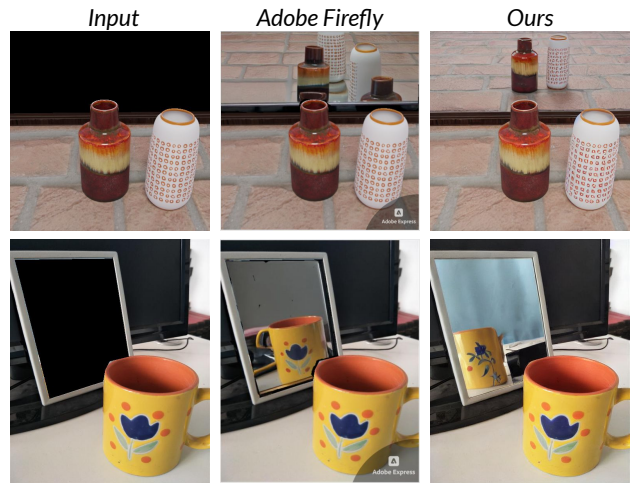


Figure 18. **Comparison with Adobe Firefly [1]**. We discuss in detail in Appendix D.6

mirror, creating an interesting visual effect where the mug appears to be floating.”

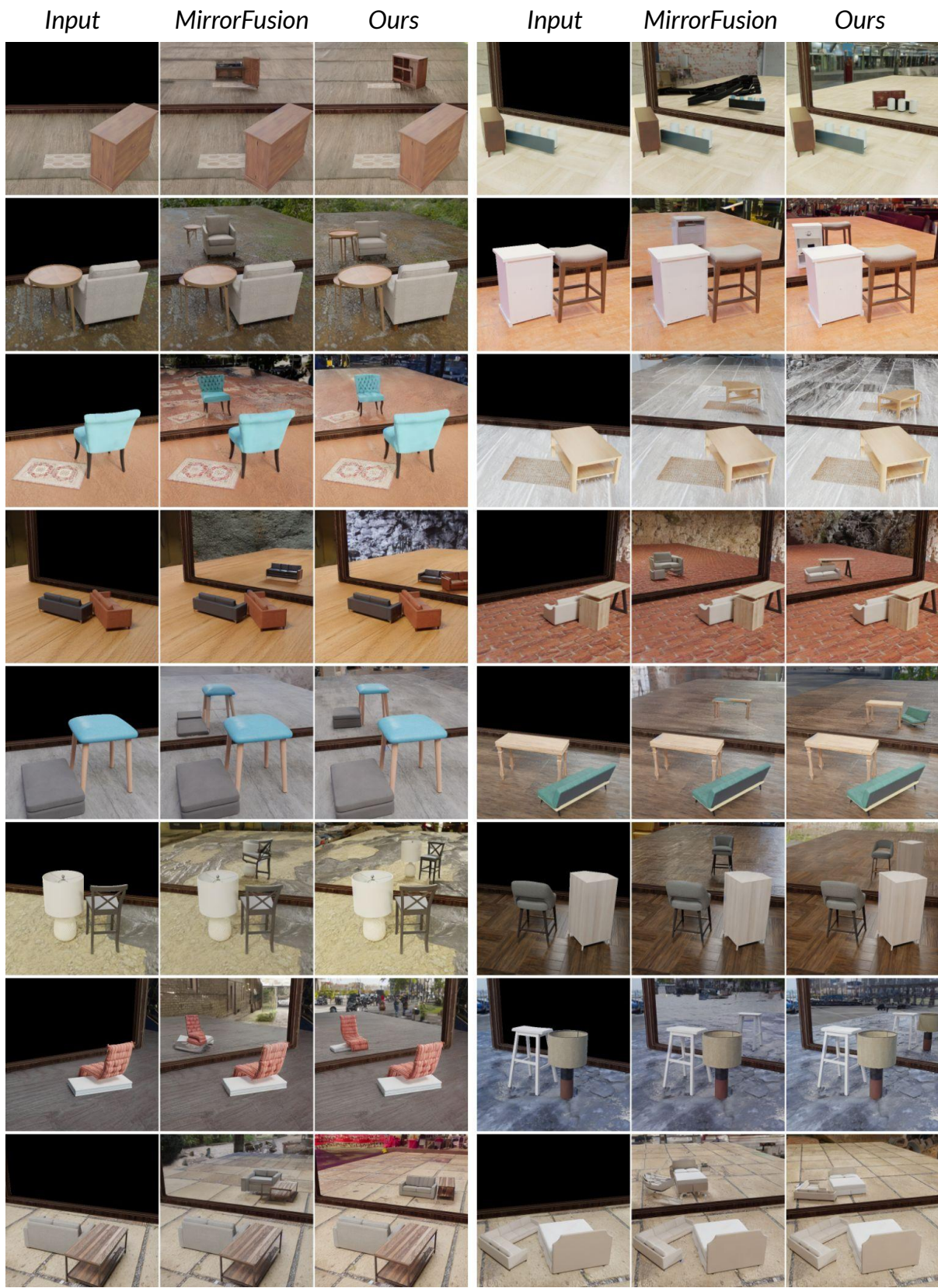


Figure 19. Results on scenes with single objects. More discussion in Appendix D.3.